

# Charge mobility of discotic mesophases: a multiscale quantum/classical study

James Kirkpatrick,<sup>1</sup> Valentina Marcon,<sup>2</sup> Jenny Nelson,<sup>1</sup> Kurt Kremer,<sup>2</sup> and Denis Andrienko<sup>2</sup>

<sup>1</sup>*Department of Physics, Imperial College London,  
Prince Consort Road, London SW7 2BW, United Kingdom*

<sup>2</sup>*Max-Planck-Institut für Polymerforschung, Ackermannweg 10, 55128 Mainz, Germany  
(Dated: September 6, 2018)*

A correlation is established between the molecular structure and charge mobility of discotic mesophases of hexabenzocoronene derivatives by combining electronic structure calculations, Molecular Dynamics, and kinetic Monte Carlo simulations. It is demonstrated that this multiscale approach can provide an accurate *ab-initio* description of charge transport in organic materials.

Organic photovoltaic (OPV) and other organic optoelectronic devices rely upon blend films of two material phases, combining the attributes of a large interfacial area for charge separation and recombination and efficient vertical transport paths. Transport in organic electronic materials proceeds by incoherent hopping and depends upon local molecular ordering as well as on the presence of percolation paths, and therefore is an intrinsically multiscale property. Improved mobilities are crucial to improved OPV device performance, and in turn require control of structure on both the intermolecular and macroscopic length scales.

Discotic liquid crystals could be ideal materials for OPV as they offer optimal design possibilities for both the charge mobility and the necessary underlying mesoscopic morphology. Discotic thermotropic liquid crystals are formed by flat molecules with a central aromatic core and aliphatic side chains [1]. They can form columnar phases, where the molecules stack on top of each other into columns, which then arrange in a regular lattice. Along the stacks of aromatic cores in the column one observes one dimensional charge transport [2, 3]. Perpendicular to the column axis the charges have to tunnel through the insulating side chains, resulting in a much reduced mobility. Therefore the discotics in a columnar phase act as nano-wires and are a promising alternative to conjugated polymers, where charge mobility in devices is often limited by inefficient inter-chain hops. Columnar mesophases could, additionally, provide for laterally segregated phases of donor and acceptor molecules with high interface areas and efficient percolation pathways. The reported high charge mobilities [2] would guarantee efficient operation. However, the spatial arrangement of stacks is never perfect: the columns can be misaligned, tilted, or form various types of topological defects, which are metastable or even stable at ambient conditions. In a recent molecular dynamics (MD) study we have shown that the degree of order in discotic stacks of hexabenzocoronene (HBC) derivatives is sensitive to the type of attached side chains [4]. The local alignment of the molecules in columns and the global arrangement of the columns in the mesophase, are thus both sensitive to molecular architecture.

A key question is the influence of local ordering in discotic mesophases on charge transport. Computer simulation is a powerful tool for probing the influence of molecular structure on charge transport. However, the task is challenging because different theoretical methods are needed to describe different length- and time-scale phenomena. Atomistic simulations are needed for local molecular arrangements [4], quantum chemical calculations are needed for the electron transfer mechanisms (and interaction with the electrodes) [5], and stochastic or rate-equation dynamic methods for simulation of charge dynamics. In this paper, we present the first statistical mechanics evaluation of the charge mobility based on quantum chemical and atomistic MD methods. We employ such a three level approach to explain the side chain dependence of charge mobility for differently substituted HBC derivatives.

Previous studies of liquid crystalline triphenylene derivatives [6] have established that polaron hopping is an appropriate description of microscopic charge transport in these materials. To use charge transport theory as a predictive, rather than descriptive tool *ab initio* calculations of the rates for charge hopping between molecules are needed. To this end we use the Marcus-Hush formalism [7] for the charge transfer rate  $\omega_{ij}$

$$\omega_{ij} = \frac{|J_{ij}|^2}{\hbar} \sqrt{\frac{\pi}{\lambda kT}} \exp \left[ -\frac{(\Delta G_{ij} - \lambda)^2}{4\lambda kT} \right], \quad (1)$$

where  $J_{ij}$  is the transfer integral for electron or hole transfer,  $\Delta G_{ij}$  the difference in free energy between the initial and final states,  $\lambda$  the reorganization energy,  $\hbar$  Planck's constant,  $k$  Boltzmann's constant and  $T$  the temperature.  $J_{ij}$  and  $\lambda$  can be computed using quantum chemical methods [5]. Note that  $J_{ij}$  is highly sensitive to the relative position and orientation of the molecules involved, which will be determined, in turn, using Molecular Dynamics. If entropic effects and energetic disorder are ignored,  $\Delta G_{ij} = \mathbf{F} \cdot \mathbf{d}_{ij}$ , where  $\mathbf{d}_{ij}$  is the vector between the center of the molecules involved in charge hopping and  $\mathbf{F}$  the electric field. In this study we choose to neglect site energy differences due to electrostatic interactions between the molecules, because such differences vanish when the conjugated cores are parallel. Further-

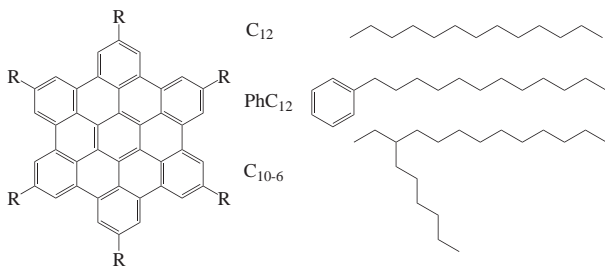


FIG. 1: Stick diagram of HBC derivatives with different side chains. We studied alkyl chains of different lengths,  $C_n$ , with  $n = 10, 12, 14, 16$ ; branched side chains,  $C_{10-6}$ ; and the dodecylphenyl-substituted side chains  $\text{PhC}_{12}$ .

more, the exclusion of site energy disorder allows us to focus exclusively on the effect of configurational disorder on charge transport, through disorder induced variations in  $J_{ij}$ .

Once all  $\omega_{ij}$  are known, charge dynamics can be simulated by Monte Carlo (MC) methods [8] or by a Master Equation (ME) approach [9]. Though several aspects of the problem are treated in the literature [10, 11], a comprehensive study on large columnar systems does not yet exist. In organic molecular crystals, Deng and coworkers [12] showed that mobilities in pentacene can be reproduced by mixed quantum chemical and molecular dynamics studies. Here we use a similar combination of methods to achieve a truly *ab-initio* description of charge mobility in HBC: (i) molecular dynamics simulations (MD) are performed on discotic mesophases of different HBC derivatives, (ii) positions and orientations of molecules are used to calculate the transfer integral  $J$  for all neighboring pairs of molecules in a column, and (iii) charge dynamics are determined using both Master Equation and kinetic MC methods.

All studied HBC derivatives are shown in Fig. 1. The molecules consist of a flat aromatic core and six side chains. Experimental data on their structural properties [2, 13, 14, 15, 16], as well as microwave conductivity (PR-TRMC) data [2, 17] are available. In some cases time-of-flight (ToF) mobility data are also available [18].

*Molecular dynamics.* In our simulation we adopt the united atom approach for the side chains, and consider explicitly only the hydrogen atoms belonging to the aromatic rings of the central core. Details of the force field and the MD setup can be found in Ref. 4. The molecules were arranged in 16 columns with 10, 20, 60, or 100 molecules in a column. Production runs of 100 ns were performed at constant pressure of 0.1 MPa and temperature  $T = 300$  K fixed using the Berendsen method with anisotropic pressure coupling. System configurations were saved every  $10^4$  MD steps (the timestep was 2 fs), yielding 200 snapshots for each run.

*Quantum Chemical Calculations.* For each MD snap-

shot, the overlap integrals  $J_{ij}$  between intracolumnar nearest neighbors  $i$  and  $j$  were calculated. To calculate  $J_{ij}$ , the aromatic core of each molecule, as output by the MD simulation, is replaced by a rigid copy of the energy minimized configuration, with the same axial and torsional orientation as the MD result. Because of molecular symmetry, the highest occupied molecular orbital (HOMO) and the lowest unoccupied molecular orbital (LUMO) of HBC are doubly occupied. Thus we have to calculate four transfer integrals for hole and four for electron transport [10]. For each component we used an adaptation of the ZINDO method, because of its speed and its insensitivity to polarization effects [19]. The effective  $J$  values are then taken as the root-mean-square of the four HOMO transfer integrals for holes and of the four LUMO transfer integrals for electrons [20]. The inner-sphere reorganization energy for cation and anion radicals was calculated using unrestricted wavefunctions, the B3LYP functional and 6-31g\*\* basis set. We found reorganization energies  $\lambda$  of 0.13 eV for cations and 0.11 eV for anions. The outer-sphere contribution was neglected.

*Kinetic MC and Master Equation (ME) simulation.* For kinetic MC, columns of molecules produced by MD are stacked periodically to produce a stack  $1 \mu\text{m}$  thick. A uniform field is applied along the stack, a charge carrier representing either an electron or a hole is introduced near one end, and the charge drift is simulated by a continuous-time random walk algorithm. The method used for MC simulation was similar to that in Ref. [21] with adjustments for a disordered lattice. The charge mobility  $\mu$  is obtained from the transit time  $t_{\text{tr}}$  of the simulated transient via  $\mu = L/Ft_{\text{tr}}$  where  $L$  is the stack thickness.  $t_{\text{tr}}$  is taken as the point of intersection of the two asymptotes to the simulated photocurrent plotted on a log-log plot, as would be done in a ToF experiment.

To compare these to steady-state mobilities along the column, we solved the linearized Master Equation [9] for continuous boundary conditions. The probability  $P_i$  of a charge being on site  $i$  obeys the rate equation:

$$\partial P_i / \partial t = \sum [ \omega_{ij} P_j - \omega_{ji} P_i ], \quad (2)$$

where the sum is over neighbors  $j \neq i$ .  $\mu$  is then obtained from the charge velocity  $\mathbf{v} = \mu \mathbf{F} = \sum_{i \neq j} (\omega_{ji} P_i - \omega_{ij} P_j) (\mathbf{r}_j - \mathbf{r}_i)$ , where  $\mathbf{r}_i$  is the coordinate of site  $i$  in the direction of  $\mathbf{F}$ .

Representative snapshots of two of the systems are shown in Fig. 2. For  $C_{12}$ , the aromatic cores are well aligned and the columns are evenly spaced whilst for  $C_{10-6}$  the branched side chains lead to a more disordered columnar structure, as studied in detail in Ref. 4. Here we mention only the parameters relevant for charge transport, namely, the intracolumnar molecular separation  $h$  and nematic order parameter  $S$ . The ordering for  $C_{10} - C_{16}$  side chains is almost perfect, while  $\text{PhC}_{12}$  and  $C_{10-6}$  are slightly more disordered. For the bulkier  $C_{10-6}$

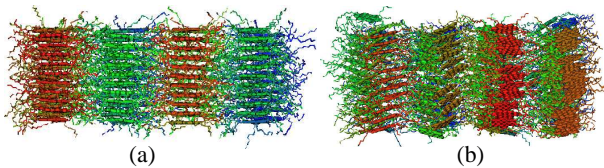


FIG. 2: MD simulation snapshots of columns of 10 HBC molecules with (a)  $C_{12}$  and (b)  $C_{10-6}$  side chains at 300 K. Columns are pre-arranged on a rectangular lattice.

we find numerous defects in the columnar arrangement. The intracolumnar separations are practically the same for all derivatives, as given in table I.

To study the effect of different side chains on mobility, we performed ToF simulations of photocurrent transients on columns constructed from copies of each MD snapshot and then averaged over results for different snapshots. This sampling method is analogous to the experimental ToF situation where charges are photogenerated in parallel columns of different configuration, and the measured transient is the sum of displacement currents from all columns. For the same  $\mathbf{F}$ ,  $t_{tr}$  varies significantly from snapshot to snapshot, *i.e.* the mobility is sensitive to the particular orientational and positional configurations of molecules in the column. Therefore, detailed tests were performed to determine the number of different columnar configurations as well as the length of the stacks needed to obtain reproducible results. Tests showed that 100 different configurations are sufficient, and for 10 molecules per column the finite size error is less than 10%.

The results of ToF simulations are shown in Fig. 3a. Comparison of the shape of the simulated transients for  $C_{10-}C_{16}$  and  $C_{10-6}$  at the same  $\mathbf{F}$  shows that the disordered  $C_{10-6}$  structures lead to relatively dispersive transients while those for  $C_{10-}C_{16}$  lead to the non-dispersive transients typical of ordered materials [22]. In our approach, where energetic disorder is neglected, disorder in charge transport can only arise from disorder in the nearest-neighbour transfer integrals  $J$ , which in turn arises from disorder in intermolecular separation and orientation. Figure 3b compares distributions of  $\log |J|^2$ . As the data clearly show, the disordered compound leads to a much wider distribution of  $J$  leading to a wider distribution of rates. In particular, the low  $J$  peak represents bottlenecks at discontinuities in the stacks, which act as traps in the one-dimensional transport.

Finally, we compare our simulations to PR-TRMC measurements. PR-TRMC probes the sum of high frequency photoinduced conductivities due to both types of charge carriers, and therefore probes the fastest contributions to charge transport, sensitive only to the local disorder within well ordered domains. PR-TRMC mobilities are therefore appropriate for comparison with our simulation since the column sizes we are using are too

compound	$\mu_{PR-TRMC}$	$\mu_{ToF}^e$	$\mu_{ToF}^h$	$\mu_{ME}^e$	$\mu_{ME}^h$	$S$	$h$
$C_{10}$	0.5 [23]	0.22	0.75	0.14	0.49	0.98	0.36
$C_{12}$	0.9 [23]	0.23	0.76	0.14	0.49	0.98	0.36
$C_{14}$	1 [23]	0.27	0.80	0.17	0.59	0.98	0.36
$C_{16}$	-	0.29	0.91	0.17	0.58	0.98	0.36
$C_{10-6}$	0.08 [17]	-	0.01	6e-4	0.003	0.96	0.37
Ph $C_{12}$	0.2 [23]	0.036	0.13	0.012	0.045	0.95	0.41

TABLE I: Electron (e) and hole (h) mobilities ( $\text{cm}^2\text{V}^{-1}\text{s}^{-1}$ ) of different compounds calculated using time-of-flight (ToF) and master equation (ME) methods, in comparison with experimentally measured PR-TRMC mobilities. Also shown are the nematic order parameter  $S$  and the average vertical separation between cores of HBC molecules  $h$  (nm).

small to include topological defects. ToF mobility data would, in contrast, be heavily dependent on defects and on fluctuations with wavelengths longer than the column size we have used. The simulated mobilities are compared with experimental data in table I and in figure 3c. The systematic overestimate of  $\mu$  by the ToF compared to the ME simulation is due to the convention used here for  $t_{tr}$ . Even though the differences in experimental PR-TRMC mobilities are relatively small, we are able to reproduce the experimental results not only qualitatively but also quantitatively. This suggests that our simulation procedure and the underlying morphologies are appropriate and that the calculated transport parameters are all in the correct order of magnitude. Of particular interest is the strong sensitivity of  $\mu$  to the degree of order in the columns, which is itself controlled by the side chain type. The highest  $\mu$  is obtained, in experiment and simulation, for the linear side-chain derivatives which also present the highest degree of intracolumnar order while the lowest  $\mu$  is obtained for the branched side-chain derivative with the least degree of order. The good correspondence between simulated and PR-TRMC mobilities arises partly from the fact that both simulation and experiment probe transport in relatively well aligned columns. To simulate ToF experiments, large systems must be studied which will require a multiscale ansatz [24].

In summary, we have determined charge mobilities of several derivatives of the discotic liquid crystal hexabenzocoronene. For the first time, three methods were combined into one scheme: (i) quantum chemical methods for the calculation of molecular electronic structures and reorganization energies (ii) molecular dynamics for simulation of the relative positions and orientations of molecules in a columnar mesophase, and (iii) kinetic Monte Carlo simulations and Master Equation approach to simulate charge transport. Applying this scheme to differently substituted HBC derivatives we are able to reproduce the trends and magnitudes of mobilities as measured by PR-TRMC. This study shows that it is possible to under-

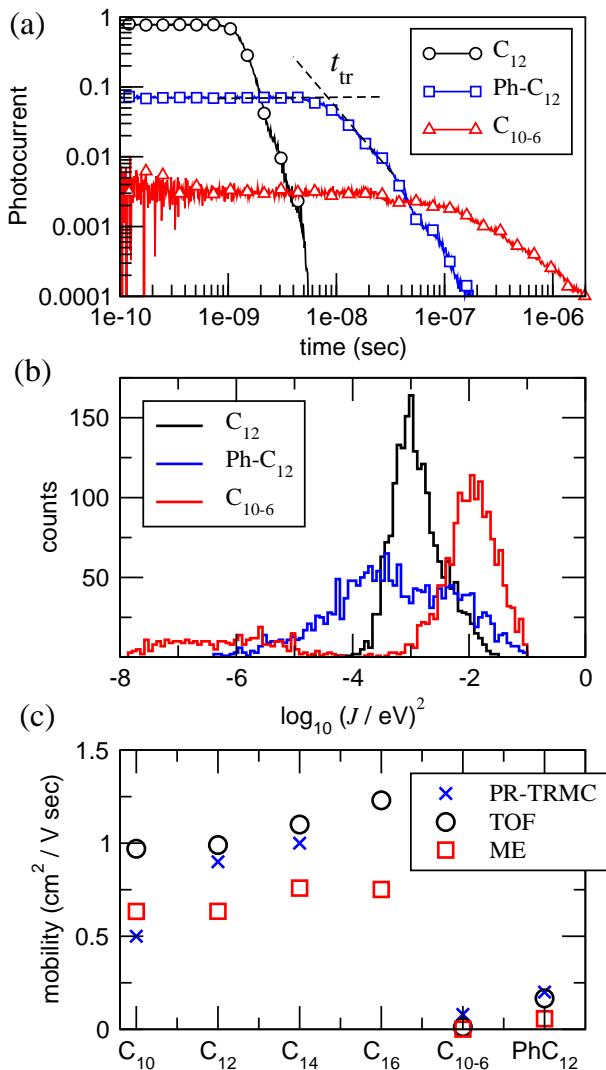


FIG. 3: (a) Simulated ToF hole photocurrent transients for C<sub>12</sub>, PhC<sub>12</sub> and C<sub>10-6</sub> at  $T = 300$  K and  $F = 10^5$  Vcm<sup>-1</sup>. Traces are averaged over 200 snapshots with columns of length 10. (b) Frequency plots of the logarithm of the transfer integral squared. In each case, results for C<sub>10</sub>-C<sub>16</sub> are practically indistinguishable from C<sub>12</sub> on the scales used. (c) Sum of electron and hole mobilities calculated by ToF and by ME, in comparison with experimental values.

stand and reproduce experimental charge transport parameters, and, in future, accurately predict them. This scheme is the outset for further studies, which will include temperature dependencies as well as solid substrates to better rationalize the self-organization of these systems. By employing multiscale schemes realistic morphologies on a semi-macroscopic scale should also become feasible.

This work was partially supported by DFG via International Research Training Group program between Germany and Korea. V.M. acknowledges AvH foundation. J.K. acknowledges the EPSRC. Discussions with K. Müllen and J. Cornil are gratefully acknowledged.

- [1] S. Chandrasekhar and G. S. Ranganath, Rep. Prog. Phys. **53**, 57 (1990).
- [2] A. M. van de Craats, J. M. Warman, A. Fechtenkotter, J. D. Brand, M. A. Harbison, and K. Müllen, Adv. Mat. **11**, 1469 (1999).
- [3] L. Schmidt-Mende, A. Fechtenkotter, K. Müllen, E. Moons, R. H. Friend, and J. D. MacKenzie, Science **293**, 1119 (2001).
- [4] D. Andrienko, V. Marcon, and K. Kremer, J. Chem. Phys. **125**, 124902 (2006).
- [5] J. L. Bredas, D. Beljonne, V. Coropceanu, and J. Cornil, Chem. Rev. **104**, 4971 (2004).
- [6] T. Kreuzis, K. Donovan, N. Boden, R. Bushby, O. Lozman, and Q. Liu, J. Chem. Phys. **114**, 1797 (2001).
- [7] K. F. Freed and J. Jortner, J. Chem. Phys. **52**, 6272 (1970).
- [8] P. Borsenberger, L. Pautmeier, and H. Bassler, J. Chem. Phys. **94**, 5447 (1991).
- [9] Z. Yu, D. Smith, A. Saxena, R. Martin, and A. Bishop, Phys. Rev. Lett. **84**, 721 (2000).
- [10] K. Senthilkumar, F. Grozema, F. Bickelhaupt, and L. Siebbeles, J. Chem. Phys. **119**, 9809 (2003).
- [11] V. Lemaure, D. Da Silva Filho, V. Coropceanu, M. Lehmann, Y. Geerts, J. Piris, M. Debije, A. Van de Craats, K. Senthilkumar, L. Siebbeles, et al., J. Am. Chem. Soc. **126**, 3271 (2004).
- [12] W. Deng and W. Goddard, J. Phys. Chem. B **108**, 8614 (2004).
- [13] I. Fischbach, T. Pakula, P. Minkin, A. Fechtenkötter, K. Müllen, H. W. Spiess, and K. Saalwächter, J. Phys. Chem. B **106**, 6408 (2002).
- [14] A. Fechtenkotter, K. Saalwachter, M. A. Harbison, K. Müllen, and H. W. Spiess, Angewandte Chemie **38**, 3039 (1999).
- [15] S. P. Brown, I. Schnell, J. D. Brand, K. Müllen, and H. W. Spiess, J. Am. Chem. Soc. **121**, 6712 (1999).
- [16] P. Herwig, C. W. Kayser, K. Müllen, and H. W. Spiess, Adv. Mat. **8**, 510 (1996).
- [17] W. Pisula, M. Kastler, D. Wasserfallen, M. Mondeshki, J. Piris, I. Schnell, and K. Müllen, Chem. Mat. **18**, 3634 (2006).
- [18] M. Kastler, W. Pisula, F. Laquai, A. Kumar, R. J. Davies, S. Balushev, M. C. Garcia-Gutiérrez, D. Wasserfallen, H. J. Butt, C. Riekel, et al., Adv. Mat. **18**, 2255 (2006).
- [19] E. Valeev, V. Coropceanu, D. da Silva, S. Salman, and J. Bredas, J. Am. Chem. Soc. **128**, 9882 (2006).
- [20] M. Newton, Chem. Rev. **91**, 767 (1991).
- [21] A. Chatten, S. M. Tuladhar, S. A. Choulis, D. D. C. Bradley, and J. Nelson, Journal of Material Science **40**, 1393 (2005).
- [22] T. Kreuzis, D. Poplavskyy, S. M. Tuladhar, M. Campoy-Quiles, J. Nelson, A. J. Campbell, and D. D. C. Bradley, Phys. Rev. B. **73**, 235201 (2006).
- [23] A. M. van de Craats, L. D. A. Siebbeles, I. Bleyl, D. Haarer, Y. A. Berlin, A. A. Zharikov, and J. M. Warman, J. Phys. Chem. B **102**, 9625 (1998).
- [24] B. Hess, S. Leon, N. van der Vegt, and K. Kremer, Soft Matter **2**, 409 (2006).